Patterns governed by chemotaxis and time delay

Mengxin Chen[1,*] and Ranchao Wu[2,†]
[1]*College of Mathematics and Information Science, Henan Normal University, Xinxiang 453007, China*
[2]*School of Mathematics and Center for Pure Mathematics, Anhui University, Hefei 230601, China*

(Received 24 April 2023; accepted 12 December 2023; published 16 January 2024)

In this paper, sufficient conditions of Turing instability are established for general delayed reaction-diffusion-chemotaxis models with no-flux boundary conditions. In particular, we address the difficulty brought about by the time delay in investigating the Turing instability. These models involve the time delay parameter τ and the general density (concentration) function in chemotaxis terms with the chemotaxis parameter χ. Theoretical results reveal that the time delay parameter τ could determine the stability of positive equilibrium for ordinary differential equations, while the chemotaxis parameter χ could describe the stability of positive equilibrium for partial differential equations. In this fashion, the general conditions of Turing instability are presented. To confirm their validity, the delayed chemotaxis-type predator-prey model and the phytoplankton-zooplankton model are considered. It is found that these two models admit Turing instability, and the numerical results are in good agreement with the theoretical analysis. The obtained results are helpful in the application of the Turing pattern in models with time delay and chemotaxis.

DOI: 10.1103/PhysRevE.109.014217

I. INTRODUCTION

Exploring the self-organizing patterns of reaction-diffusion models is still an interesting topic. Turing [1] proposed a mechanism to explain how cell signaling can generate self-organizing patterns. The self-organizing pattern will emerge in reaction-diffusion models when the parameters lie in the Turing domain. To be precise, the constant steady state is stable for the spatially homogeneous system, while it will become unstable for the spatially inhomogeneous system. Typically, this is Turing instability or diffusion-driven instability. Over the years, a large number of reaction-diffusion models have been employed to investigate the pattern formation induced by Turing instability. By using the Gierer-Meinhardt model, Chen *et al.* [2] reported Turing instability and exhibited the spot pattern, the mixed pattern, and higher-order instabilities near the Turing onset. Gorder *et al.* [3] obtained general conditions for the onset and structure of diffusion-driven instabilities in reaction-diffusion systems, and they demonstrated the general Turing conditions on a variety of domains with different evolution laws. Butler and Goldenfeld [4] illustrated that the inclusion of intrinsic noise will lead to the formation of "quasipatterns," and such a pattern phenomenon is experimentally distinguishable from the standard Turing patterns. Xiang *et al.* [5] investigated the Turing patterns with high resolution formed without chemical reaction in a thin-film solution of organic semiconductors, and they gave multiple regular patterns with micro/nanometer-scale features, such as line, square-grid, zigzag, and fencelike patterns, etc. See also Refs. [6–11].

As we know, time delay widely exists in the process of population dynamics, and it may also be the potential factor for the emergence of pattern formation [12–16]. The corresponding dynamic profiles do not appear immediately for some reason. For example, large-scale outbreaks of infectious diseases always take a while since the infected individual needs an exposure period to show symptoms. Consequently, time delay describes the dynamic profiles that depend not only on the state at time t, but also that moment before t due to some factors from a practical point of view. On the other hand, chemotaxis reflects the directed movement of the species according to the concentrations or densities of the chemical substance or populations. The first chemotaxis model was proposed by Keller and Segel [17] to describe the aggregation of a certain type of bacteria. Since then, many chemotaxis models have been proposed and studied to clarify the dynamic behaviors among the species; see Refs. [18–24], etc. It is suggested that the model with chemotaxis could display rich dynamical phenomena.

However, few results have been reported about pattern formation in models with chemotaxis and time delay based on Turing instability. The problem is that the characteristic equation at equilibrium is a transcendental equation, which makes it difficult to find the emergence conditions of the Turing instability. In this present work, we investigate a general reaction-diffusion model with nonlinear chemotaxis and time delay in kinetics terms. By applying and extending the method in [25], we will eliminate the time delay terms and give the general occurrence conditions of Turing instability. In this manner, we can overcome the difficulty induced by the transcendental equation. Our theoretical results illustrate that time delay will govern the stability of the spatially homogeneous model, while the chemotaxis sensitivity coefficient will determine the stability of the spatially

*chmxdc@163.com
†Corresponding author: rcwu@ahu.edu.cn

inhomogeneous model. As a consequence, Turing instability may occur when we adjust the ranges of the time delay parameter and chemotaxis sensitivity coefficient. Two examples are given to check the theoretical prediction. Note that these models will admit pattern formation due to the existence of Turing instability. Of course, our techniques and results can be used in other reaction-diffusion models with time delay and chemotaxis.

II. GENERAL CONDITIONS FOR TURING INSTABILITY

Consider the following general reaction-diffusion-chemotaxis model with zero-flux boundary conditions:

$$\begin{aligned}
&\frac{\partial u}{\partial t} = d_1\Delta u + f(u(x,t-\tau), v(x,t-\tau)), \quad x\in\Omega,\ t>0,\\
&\frac{\partial v}{\partial t} = d_2\Delta v - \nabla\cdot[\chi\phi(v)\nabla u] + g(u(x,t-\tau), v(x,t-\tau)), \quad x\in\Omega,\ t>0,\\
&\frac{\partial u}{\partial \nu} = \frac{\partial v}{\partial \nu} = 0, \quad x\in\partial\Omega,\ t\geqslant 0,\\
&u(x,t) = u_0(x,t)\geqslant 0,\ v(x,t) = v_0(x,t)\geqslant 0, \quad x\in\Omega,\ t\in[-\tau,0],
\end{aligned} \tag{1}$$

where u and v are the densities of two species; functions f and g represent reaction kinetics terms; positive constants d_1 and d_2 are diffusion rates of u and v, respectively; $\Omega\subset\mathbb{R}$ is a bounded domain; ν is the outward unit normal vector along the smooth boundary $\partial\Omega$; $\tau>0$ implies time delay; and $u_0(x,t)\geqslant 0$ and $v_0(x,t)\geqslant 0$ imply the initial concentrations (densities) of u and v, respectively. The term $-\nabla\cdot[\chi\phi(v)\nabla u]$ is the chemotaxis term, and it means that they will move preferentially toward patches with the highest density of u as $\chi>0$, and v will move toward the opposite direction of u when $\chi<0$. So, we claim that χ describes the sensitivity coefficient, and $\phi(v)$ are the density functions with respect to v. Generally, $\phi(v)$ could take the following forms. (i) Linear form [22,26]: $\phi(v)=v$; (ii) saturated form [27]: $\phi(v)=\frac{v}{1+\epsilon v^m}$ with $\epsilon>0$ and $m\geqslant 1$; (iii) Ricker form [27]: $\phi(v)=ve^{-\epsilon v}$ with $\epsilon>0$; (iv) monotonic nonincreasing form [28,29]: $\phi(v)=\frac{1}{1+v}$ or $\phi(v)=\frac{1}{(1+v)^2}$.

From the original idea of Sen *et al.* [25], we set $u(x,t-\tau)=u(x,t)-\tau\frac{\partial u(x,t)}{\partial t}$, $v(x,t-\tau)=v(x,t)-\tau\frac{\partial v(x,t)}{\partial t}$. Consequently, by putting them into (1), we get

$$\begin{aligned}
&\frac{\partial u}{\partial t} = d_1\Delta u + f\left(u(x,t)-\tau\frac{\partial u(x,t)}{\partial t}, v(x,t)-\tau\frac{\partial v(x,t)}{\partial t}\right), \quad x\in\Omega,\ t>0,\\
&\frac{\partial v}{\partial t} = d_2\Delta v - \nabla\cdot[\chi\phi(v)\nabla u] + g\left(u(x,t)-\tau\frac{\partial u(x,t)}{\partial t}, v(x,t)-\tau\frac{\partial v(x,t)}{\partial t}\right), \quad x\in\Omega,\ t>0,\\
&\frac{\partial u}{\partial \nu} = \frac{\partial v}{\partial \nu} = 0, \quad x\in\partial\Omega,\ t\geqslant 0,\\
&u(x,t) = u_0(x)\geqslant 0,\ v(x,t) = v_0(x)\geqslant 0, \quad x\in\Omega.
\end{aligned} \tag{2}$$

Now expanding the terms f and g in (2), we obtain

$$f\left(u-\tau\frac{\partial u}{\partial t}, v-\tau\frac{\partial v}{\partial t}\right) = f(u,v) - \tau f'_u\frac{\partial u}{\partial t} - \tau f'_v\frac{\partial v}{\partial t} + \tau^2\frac{f'_{uu}}{2}\left(\frac{\partial u}{\partial t}\right)^2 + \tau^2 f'_{uv}\frac{\partial u}{\partial t}\frac{\partial v}{\partial t} + \tau^2\frac{f'_{vv}}{2}\left(\frac{\partial v}{\partial t}\right)^2 + \cdots$$

and

$$g\left(u-\tau\frac{\partial u}{\partial t}, v-\tau\frac{\partial v}{\partial t}\right) = g(u,v) - \tau g'_u\frac{\partial u}{\partial t} - \tau g'_v\frac{\partial v}{\partial t} + \tau^2\frac{g'_{uu}}{2}\left(\frac{\partial u}{\partial t}\right)^2 + \tau^2 g'_{uv}\frac{\partial u}{\partial t}\frac{\partial v}{\partial t} + \tau^2\frac{g'_{vv}}{2}\left(\frac{\partial v}{\partial t}\right)^2 + \cdots.$$

Neglecting the higher-order nonlinear terms, one yields

$$f\left(u-\tau\frac{\partial u}{\partial t}, v-\tau\frac{\partial v}{\partial t}\right) \approx f(u,v) - \tau f'_u\frac{\partial u}{\partial t} - \tau f'_v\frac{\partial v}{\partial t} \tag{3}$$

and

$$g\left(u-\tau\frac{\partial u}{\partial t}, v-\tau\frac{\partial v}{\partial t}\right) \approx g(u,v) - \tau g'_u\frac{\partial u}{\partial t} - \tau g'_v\frac{\partial v}{\partial t}. \tag{4}$$

As such, by putting (3) and (4) into (2), we get

$$\begin{aligned}
\frac{\partial u}{\partial t} &= d_1\Delta u + f(u,v) - \tau f'_u\frac{\partial u}{\partial t} - \tau f'_v\frac{\partial v}{\partial t},\\
\frac{\partial v}{\partial t} &= d_2\Delta v - \nabla\cdot[\chi\phi(v)\nabla u] + g(u,v)\\
&\quad - \tau g'_u\frac{\partial u}{\partial t} - \tau g'_v\frac{\partial v}{\partial t}.
\end{aligned} \tag{5}$$

For the solution (u, v) of model (5), consider its small perturbation $u = u_* + \epsilon u$ and $v = v_* + \epsilon v$, where we assume that (u_*, v_*) is a positive equilibrium of model (5). This gives $f(u_*, v_*) = 0$ and $g(u_*, v_*) = 0$. Consequently, Taylor-expanding $f(u, v)$, $g(u, v)$, and $\phi(v)$ around (u_*, v_*), one has

$$\begin{aligned}\phi(v) &= \phi(v_*) + \phi_v(\epsilon v) + \tfrac{1}{2}\phi_{vv}(\epsilon v)^2 + \cdots,\\ f(u, v) &= f(u_*, v_*) + f_u(\epsilon u) + f_v(\epsilon v) + \tfrac{1}{2}f_{uu}(\epsilon u)^2\\ &\quad + f_{uv}(\epsilon u)(\epsilon v) + \tfrac{1}{2}f_{vv}(\epsilon v)^2 + \cdots,\\ g(u, v) &= g(u_*, v_*) + g_u(\epsilon u) + g_v(\epsilon v) + \tfrac{1}{2}g_{uu}(\epsilon u)^2\\ &\quad + g_{uv}(\epsilon u)(\epsilon v) + \tfrac{1}{2}g_{vv}(\epsilon v)^2 + \cdots. \end{aligned} \tag{6}$$

It is noticed that $f(u_*, v_*) = 0$ and $g(u_*, v_*) = 0$. Equations (6) then become

$$\begin{aligned}\phi(v) &= \phi(v_*) + \phi_v(\epsilon v) + \tfrac{1}{2}\phi_{vv}(\epsilon v)^2 + \cdots,\\ f(u, v) &= f_u(\epsilon u) + f_v(\epsilon v) + \tfrac{1}{2}f_{uu}(\epsilon u)^2\\ &\quad + f_{uv}(\epsilon u)(\epsilon v) + \tfrac{1}{2}f_{vv}(\epsilon v)^2 + \cdots,\\ g(u, v) &= g_u(\epsilon u) + g_v(\epsilon v) + \tfrac{1}{2}g_{uu}(\epsilon u)^2\\ &\quad + g_{uv}(\epsilon u)(\epsilon v) + \tfrac{1}{2}g_{vv}(\epsilon v)^2 + \cdots. \end{aligned} \tag{7}$$

So the first-order terms of (7) enjoy

$$\begin{aligned}\phi(v) &\approx \phi(v_*) + \phi_v(\epsilon v),\\ f(u, v) &\approx f_u(\epsilon u) + f_v(\epsilon v),\\ g(u, v) &\approx g_u(\epsilon u) + g_v(\epsilon v). \end{aligned} \tag{8}$$

Then around (u_*, v_*), putting (8) into (5), we have

$$\begin{aligned}(1 + \tau f_u)\frac{\partial \epsilon u}{\partial t} + \tau f_v \frac{\partial \epsilon v}{\partial t} &= d_1 \Delta \epsilon u + f_u(\epsilon u) + f_v(\epsilon v),\\ \tau g_u \frac{\partial \epsilon u}{\partial t} + (1 + \tau g_v)\frac{\partial \epsilon v}{\partial t} &= d_2 \Delta \epsilon v - \chi \phi(v_*)\Delta \epsilon u\\ &\quad + g_u(\epsilon u) + g_v(\epsilon v), \end{aligned} \tag{9}$$

where $f_u = f_u'|_{(u_*, v_*)}$, $f_v = f_v'|_{(u_*, v_*)}$, $g_u = g_u'|_{(u_*, v_*)}$, $g_v = g_v'|_{(u_*, v_*)}$, and we employ

$$\begin{aligned}&\nabla \cdot \{[\phi(v_*) + \phi_v(\epsilon v)]\nabla \epsilon u\}\\ &\quad = \nabla \phi_v(v - v_*) \cdot \nabla \epsilon u\\ &\qquad + [\phi(v_*) + \phi_v(v - v_*)]\Delta \epsilon u\\ &\quad = \phi(v_*)\Delta \epsilon u \end{aligned}$$

at the positive equilibrium (u_*, v_*). Thereby, we have

$$A_\tau \begin{pmatrix} \epsilon u_t \\ \epsilon v_t \end{pmatrix} = D \begin{pmatrix} \epsilon u \\ \epsilon v \end{pmatrix} + J_0 \begin{pmatrix} \epsilon u \\ \epsilon v \end{pmatrix}, \tag{10}$$

where $A_\tau = \begin{pmatrix} 1 + \tau f_u & \tau f_v \\ \tau g_u & 1 + \tau g_v \end{pmatrix}$ and

$$D = \begin{pmatrix} d_1 \Delta & 0 \\ -\chi \phi(v_*)\Delta & d_2 \Delta \end{pmatrix}, \quad J_0 = \begin{pmatrix} f_u & f_v \\ g_u & g_v \end{pmatrix}.$$

Suppose that the solution $(\epsilon u, \epsilon v)$ takes the form

$$\begin{pmatrix} \epsilon u \\ \epsilon v \end{pmatrix} = \sum_{k=0}^{\infty} \begin{pmatrix} a_k \\ b_k \end{pmatrix} e^{\lambda_k t} \cos kx,$$

where a_k, b_k are constants, λ_k is the temporal spectrum, and k represents the spatial spectrum. Then from (10), we have

$$\begin{aligned}&\lambda_k \begin{pmatrix} 1 + \tau f_u & \tau f_v \\ \tau g_u & 1 + \tau g_v \end{pmatrix} \sum_{k=0}^{\infty} \begin{pmatrix} a_k \\ b_k \end{pmatrix} e^{\lambda_k t} \cos kx\\ &\quad = \begin{pmatrix} -d_1 k^2 + f_u & f_v \\ \chi \phi(v_*)k^2 + g_u & -d_2 k^2 + g_v \end{pmatrix} \sum_{k=0}^{\infty} \begin{pmatrix} a_k \\ b_k \end{pmatrix} e^{\lambda_k t} \cos kx. \end{aligned}$$

Accordingly, one obtains

$$\begin{vmatrix} \lambda_k(1 + \tau f_u) + d_1 k^2 - f_u & (\lambda_k \tau - 1) f_v \\ (\lambda_k \tau - 1) g_u - \chi \phi(v_*)k^2 & \lambda_k(1 + \tau g_v) + d_2 k^2 - g_v \end{vmatrix} = 0.$$

For small time delay parameter $\tau > 0$, we neglect the higher-order nonlinearities of $O(\tau^2)$. In this fashion, we get the characteristic equation as follows:

$$\lambda_k^2 - T_k(\tau, \chi)\lambda_k + D_k(\tau, \chi) = 0, \quad k \in \mathbb{N}_0 = \{0, 1, 2, \dots\}, \tag{11}$$

where

$$\begin{aligned}T_k(\tau, \chi) &= \frac{-\{[d_2 f_u + d_1 g_v + \chi \phi(v_*) f_v]\tau + d_1 + d_2\}k^2}{(g_v + f_u)\tau + 1}\\ &\quad + T_0(\tau, \chi) \end{aligned}$$

and

$$\begin{aligned}D_k(\tau, \chi) &= \frac{d_1 d_2 k^4 - [d_1 g_v + d_2 f_u + \chi \phi(v_*) f_v]k^2}{(g_v + f_u)\tau + 1}\\ &\quad + D_0(\tau, \chi), \end{aligned}$$

with

$$T_0(\tau, \chi) = \frac{g_v + f_u + 2\tau(f_u g_v - f_v g_u)}{(g_v + f_u)\tau + 1}$$

and

$$D_0(\tau, \chi) = \frac{f_u g_v - f_v g_u}{(g_v + f_u)\tau + 1}.$$

If $k = 0$, one has

$$\lambda_0^2 - T_0(\tau, \chi)\lambda_0 + D_0(\tau, \chi) = 0. \tag{12}$$

Obviously, (12) is the characteristic equation of the spatially homogeneous model around the positive equilibrium (u_*, v_*). Our following task is to find the occurrence conditions of Turing instability.

For the Turing instability of the reaction-diffusion-chemotaxis model (1), we first should ensure that the positive equilibrium (u_*, v_*) is locally asymptotically stable for its spatially homogeneous model, and then it becomes unstable when the diffusion and chemotaxis are present. Keeping this in mind, we first discuss the stability of the positive equilibrium (u_*, v_*) by investigating the characteristic equation (12). Now an easy analysis reveals that the positive equilibrium (u_*, v_*) is locally asymptotically stable when $T_0(\tau, \chi) < 0$ and $D_0(\tau, \chi) > 0$ are valid. If $f_u g_v - f_v g_u < 0$ and $(g_v + f_u)\tau + 1 < 0$, we immediately obtain that $T_0(\tau, \chi) > 0$ and $D_0(\tau, \chi) > 0$ hold. This implies that all the real parts of the eigenvalues of the characteristic equation (12) are greater than zero, so the positive equilibrium (u_*, v_*) is unstable. Now if $f_u g_v - f_v g_u > 0$ and $(g_v + f_u)\tau + 1 > 0$ are satisfied,

we have $D_0(\tau,\chi)>0$. Moreover, if we restrict $g_v+f_u+2\tau(f_ug_v-f_vg_u)<0$, then one claims that $T_0(\tau,\chi)<0$ is true. Consequently, the positive equilibrium (u_*,v_*) is locally asymptotically stable if the following condition is valid:

$$0<\tau<\min\left\{-\frac{1}{g_v+f_u},-\frac{g_v+f_u}{2(f_ug_v-f_vg_u)}\right\}. \tag{13}$$

Obviously, (13) implies that $g_v+f_u<0$ spontaneously holds.

In the sequel, we shall find some conditions such that the positive equilibrium (u_*,v_*) is unstable when diffusion and chemotaxis are present and (13) is true.

It is noticed that

$$T_k(\tau,\chi)=\frac{-\{[d_2f_u+d_1g_v+\chi\phi(v_*)f_v]\tau+d_1+d_2\}k^2}{(g_v+f_u)\tau+1}+T_0(\tau,\chi),$$

where $T_0(\tau,\chi)<0$ and $(g_v+f_u)\tau+1>0$ due to (13). As a result, if $[d_2f_u+d_1g_v+\chi\phi(v_*)f_v]\tau+d_1+d_2>0$, this is $\chi<-\frac{(d_1g_v+d_2f_u)\tau+d_1+d_2}{\phi(v_*)f_v\tau}:=\chi^*$ for $f_v<0$ or $\chi>-\frac{(d_1g_v+d_2f_u)\tau+d_1+d_2}{\phi(v_*)f_v\tau}:=\chi_*$ for $f_v>0$, and we infer that $T_k(\tau,\chi)<0$ for all $k\in\mathbb{N}_0/\{0\}$. Thereby, the stability of the positive equilibrium E_* only depends on the sign of $D_k(\tau,\chi)$. If $H(k^2)=d_1d_2k^4-[d_1g_v+d_2f_u+\chi\phi(v_*)f_v]k^2+f_ug_v-f_vg_u$, this gives $D_k(\tau,\chi)=\frac{H(k^2)}{(g_v+f_u)\tau+1}$. So we claim that $\mathrm{sgn}(D_k(\tau,\chi))=\mathrm{sgn}(H(k^2))$, since $(g_v+f_u)\tau+1>0$ is valid. Denoting by $z=k^2$, this implies that $H(z)=d_1d_2z^2-[d_1g_v+d_2f_u+\chi\phi(v_*)f_v]z+f_ug_v-f_vg_u$. Let us find the sign of $H(z)$ for $z\in(0,\infty)$. Since $\min_{z>0}H(z)=0$, then $\min_{z>0}H(z)=-h(\chi)=0$ with

$$h(\chi)=\phi^2(v_*)f_v^2\chi^2+2\phi(v_*)f_v(d_1g_v+d_2f_u)\chi+(d_1g_v-d_2f_u)^2+4d_1d_2f_vg_u.$$

A direct computation suggests that the root's discriminant of $h(\chi)=0$ is $16\phi^2(v_*)f_v^2d_1d_2(f_ug_v-f_vg_u)>0$. Hence, $h(\chi)=0$ must have two real roots. We have the following cases with respect to the roots of $h(\chi)=0$.

(I) If $f_v(d_1g_v+d_2f_u)<0$ and $(d_1g_v-d_2f_u)^2+4d_1d_2f_vg_u>0$, then $h(\chi)=0$ has two positive roots,

$$\chi_1=\frac{-(d_1g_v+d_2f_u)f_v-2|f_v|\sqrt{d_1d_2(f_ug_v-f_vg_u)}}{\phi(v_*)f_v^2}>0$$

and

$$\chi_2=\frac{-(d_1g_v+d_2f_u)f_v+2|f_v|\sqrt{d_1d_2(f_ug_v-f_vg_u)}}{\phi(v_*)f_v^2}>0.$$

Consequently, $h(\chi)>0$ if $\chi<\chi_1$ or $\chi>\chi_2$ and $h(\chi)<0$ if $\chi_1<\chi<\chi_2$ is valid. Since $\min_{z>0}H(z)=-h(\chi)=0$, we obtain $H(k^2)>0$ if $\chi_1<\chi<\chi_2$ and $H(k^2)<0$ if $\chi<\chi_1$ or $\chi>\chi_2$ for some $k\in\mathbb{N}_0/\{0\}$. As a result, if $f_v<0$ and $\chi_1<\chi<\min\{\chi^*,\chi_2\}$, then the positive equilibrium (u_*,v_*) is locally asymptotically stable and there is no Turing instability. If $f_v<0$ and $\chi<\min\{\chi^*,\chi_1\}$ or $f_v<0$ and $\chi_2<\chi<\chi^*$, then the positive equilibrium (u_*,v_*) is unstable and there is Turing instability. Similarly, if $f_v>0$ and $\max\{\chi_*,\chi_1\}<\chi<\chi_2$, then the positive equilibrium (u_*,v_*) is locally asymptotically stable and there is no Turing instability. However, if $f_v>0$ and $\chi>\max\{\chi_*,\chi_2\}$ or $f_v>0$ and $\chi_*<\chi<\chi_1$, then the positive equilibrium (u_*,v_*) is unstable and there is Turing instability.

(II) If $(d_1g_v-d_2f_u)^2+4d_1d_2f_vg_u\leqslant 0$, then $h(\chi)=0$ has a negative root and a positive root,

$$\chi_3=\frac{-(d_1g_v+d_2f_u)f_v-2|f_v|\sqrt{d_1d_2(f_ug_v-f_vg_u)}}{\phi(v_*)f_v^2}<0$$

and

$$\chi_4=\frac{-(d_1g_v+d_2f_u)f_v+2|f_v|\sqrt{d_1d_2(f_ug_v-f_vg_u)}}{\phi(v_*)f_v^2}>0.$$

We find that $h(\chi)>0$ if $\chi<\chi_3$ or $\chi>\chi_4$ and $h(\chi)<0$ if $\chi_3<\chi<\chi_4$ holds. These imply that $H(k^2)>0$ if $\chi_3<\chi<\chi_4$ and $H(k^2)<0$ if $\chi<\chi_3$ or $\chi>\chi_4$ for some $k\in\mathbb{N}_0/\{0\}$. Thereby, if $f_v<0$ and $\chi_3<\chi<\min\{\chi^*,\chi_4\}$, then the positive equilibrium (u_*,v_*) is locally asymptotically stable and there is no Turing instability. If $f_v<0$ and $\chi<\min\{\chi^*,\chi_3\}$ or $f_v<0$ and $\chi_4<\chi<\chi^*$, then the positive equilibrium (u_*,v_*) is unstable and there is Turing instability. In a similar fashion, if $f_v>0$ and $\max\{\chi_*,\chi_3\}<\chi<\chi_4$, then the positive equilibrium (u_*,v_*) is locally asymptotically stable and there is no Turing instability, while if $f_v>0$ and $\chi>\max\{\chi_*,\chi_4\}$ or $f_v>0$ and $\chi_*<\chi<\chi_3$, then (u_*,v_*) is unstable and there is Turing instability.

(III) If $f_v(d_1g_v+d_2f_u)>0$ and $(d_1g_v-d_2f_u)^2+4d_1d_2f_vg_u>0$, $h(\chi)=0$ has two negative roots,

$$\chi_5=\frac{-(d_1g_v+d_2f_u)f_v-2|f_v|\sqrt{d_1d_2(f_ug_v-f_vg_u)}}{\phi(v_*)f_v^2}<0$$

and

$$\chi_6=\frac{-(d_1g_v+d_2f_u)f_v+2|f_v|\sqrt{d_1d_2(f_ug_v-f_vg_u)}}{\phi(v_*)f_v^2}<0.$$

We can confirm that if $f_v<0$ and $\chi_5<\chi<\min\{\chi^*,\chi_6\}$, then the positive equilibrium (u_*,v_*) is locally asymptotically stable and there is no Turing instability. If $f_v<0$ and $\chi<\min\{\chi^*,\chi_5\}$ or $f_v<0$ and $\chi_6<\chi<\chi^*$, then the positive equilibrium (u_*,v_*) is unstable and there is Turing instability. On the other hand, if $f_v>0$ and $\max\{\chi_*,\chi_5\}<\chi<\chi_6$, then the positive equilibrium (u_*,v_*) is locally asymptotically stable and there is no Turing instability. However, if $f_v>0$ and $\chi>\max\{\chi_*,\chi_6\}$ or $f_v>0$ and $\chi_*<\chi<\chi_5$, then (u_*,v_*) is unstable and there is Turing instability.

Now let us determine the critical wave number, say k_c, of the Turing instability. Using $\min_{z>0}H(z)=\min_{k^2>0}H(k^2)=0$, we immediately obtain $k_c^2=\sqrt{\frac{f_ug_v-f_vg_u}{d_1d_2}}>0$.

To summarize, we build the following stability result:

Theorem 1. Supposing that (u_*,v_*) is a positive equilibrium of the reaction-diffusion-chemotaxis model (1) and

$$0<\tau<\min\left\{-\frac{1}{g_v+f_u},-\frac{g_v+f_u}{2(f_ug_v-f_vg_u)}\right\},$$

we have the following:

(i) If $f_v<0$ and $\chi_L^c<\chi<\min\{\chi^*,\chi_R^c\}$, then (u_*,v_*) is locally asymptotically stable.

(ii) If $f_v<0$ and $\chi<\min\{\chi^*,\chi_L^c\}$ or $\chi_R^c<\chi<\chi^*$, then Turing instability exists with the critical wave number $k=k_c$.

(iii) If $f_v>0$ and $\max\{\chi_*,\chi_L^c\}<\chi<\chi_R^c$, then (u_*,v_*) is locally asymptotically stable.

(iv) If $f_v > 0$ and $\chi > \max\{\chi_*, \chi_R^c\}$ or $\chi_* < \chi < \chi_L^c$, then Turing instability exists with the critical wave number $k = k_c$, where k_c enjoys $k_c^2 = \sqrt{\frac{f_u g_v - f_v g_u}{d_1 d_2}} > 0$, $\chi_L^c \in \{\chi_1, \chi_3, \chi_5\}$, and $\chi_R^c \in \{\chi_2, \chi_4, \chi_6\}$.

Remark 1. From Theorem 1, we find that the time delay parameter τ could determine the stability of the positive equilibrium for ordinary differential equations (ODEs), while the chemotaxis coefficient χ could control the stability of the positive equilibrium for partial differential equations (PDEs). Hence, we can yield the parameter ranges for the Turing instability by adjusting τ and χ.

III. SOME APPLICATIONS

A. Delayed predator-prey model with chemotaxis

Consider the following predator-prey model:

$$\begin{aligned}
\frac{\partial u}{\partial t} &= d_1 \Delta u + u(1 - bu - v_\tau), \\
\frac{\partial v}{\partial t} &= d_2 \Delta v - \chi \nabla \cdot [\phi(v) \nabla u] + v(u - c), \\
\frac{\partial u}{\partial \nu} &= \frac{\partial v}{\partial \nu} = 0, \\
u(x,t) &= u_0(x,t) \geqslant 0, \\
v(x,t) &= v_0(x,t) \geqslant 0,
\end{aligned} \tag{14}$$

where u and v are the densities of the prey and predator; d_1 and d_2 are the diffusion rates of u and v, respectively; $v_\tau = v(x, t - \tau)$ with time delay $\tau > 0$; and b and c are two positive constants. The term $-\chi \nabla \cdot [\phi(v) \nabla u]$ is the chemotaxis term, and it implies the predator will move toward the positive and the opposite directions of a high density of prey as the chemotaxis coefficient $\chi > 0$ (attractive chemotaxis) and $\chi < 0$ (repulsive chemotaxis), respectively. We recommend the existing literature [22,30] for some known dynamic results with respect to (14) without time delay or chemotaxis.

We can confirm that $(u_*, v_*) = (c, 1 - bc)$, with $0 < bc < 1$ a positive equilibrium of (14). Denoting $f(u, v) = u(1 - bu - v)$ and $g(u, v) = v(u - c)$, we obtain $f_u = -bc$, $f_v = -c$, $g_u = 1 - bc$, and $g_v = 0$. Now putting $v(x, t - \tau) = v(x, t) - \tau \frac{\partial v(x,t)}{\partial t}$ into (14), and by using (9), we get the linearization form of (14) as follows:

$$\begin{aligned}
\frac{\partial u}{\partial t} - \tau c \frac{\partial v}{\partial t} &= d_1 \Delta u - bcu - cv, \\
\frac{\partial v}{\partial t} &= d_2 \Delta v - \chi \phi(v_*) \Delta u + (1 - bc)u.
\end{aligned}$$

Consequently, we have $A_\tau = \left(\begin{smallmatrix} 1 & -\tau c \\ 0 & 1 \end{smallmatrix}\right)$ and

$$D = \begin{pmatrix} d_1 \Delta & 0 \\ -\chi \phi(v_*) \Delta & d_2 \Delta \end{pmatrix}, \; J_0 = \begin{pmatrix} -bc & -c \\ 1 - bc & 0 \end{pmatrix}.$$

Consider the following general solution:

$$\begin{pmatrix} u \\ v \end{pmatrix} = \sum_{k=0}^{\infty} \begin{pmatrix} a_k \\ b_k \end{pmatrix} e^{\lambda_k t} \cos kx,$$

where a_k, b_k are constants, λ_k is the temporal spectrum, and k represents the spatial spectrum. Then

$$\begin{aligned}
&\lambda_k \begin{pmatrix} 1 & -\tau c \\ 0 & 1 \end{pmatrix} \sum_{k=0}^{\infty} \begin{pmatrix} a_k \\ b_k \end{pmatrix} e^{\lambda_k t} \cos kx \\
&= \begin{pmatrix} -d_1 k^2 - bc & -c \\ \chi \phi(v_*) k^2 + 1 - bc & -d_2 k^2 \end{pmatrix} \sum_{k=0}^{\infty} \begin{pmatrix} a_k \\ b_k \end{pmatrix} e^{\lambda_k t} \cos kx.
\end{aligned}$$

Accordingly, one obtains the characteristic equation

$$\lambda_k^2 - T_k(\tau, \chi)\lambda_k + D_k(\tau, \chi) = 0, \; k \in \mathbb{N}_0,$$

where

$$T_k(\tau, \chi) = [\chi \phi(v_*) c\tau - d_1 - d_2]k^2 - bc + c\tau(1 - bc)$$

and

$$D_k(\tau, \chi) = d_1 d_2 k^4 + [bcd_2 + \chi \phi(v_*) c]k^2 + c(1 - bc).$$

If $k = 0$, one has

$$\lambda_0^2 - T_0(\tau, \chi)\lambda_0 + D_0(\tau, \chi) = 0,$$

where

$$T_0(\tau, \chi) = -bc + c\tau(1 - bc), \; D_0(\tau, \chi) = c(1 - bc) > 0.$$

Therefore, the unique positive equilibrium $(u_*, v_*) = (c, 1 - bc)$ is locally asymptotically stable if we restrict $0 < \tau < \frac{b}{1 - bc}$. Moreover, we have $\chi^* = \frac{d_1 + d_2}{\phi(v_*) c\tau} > 0$ and $f_v = -c < 0$.

Then from Theorem 1, one yields the following result:

Theorem 2. For the reaction-diffusion-chemotaxis model (14), suppose that

$$0 < \tau < \frac{b}{1 - bc}.$$

We have the following:

(i) If $\frac{-bcd_2 - 2\sqrt{d_1 d_2 c(1-bc)}}{\phi(v_*)c} < \chi < \min\{\frac{d_1 + d_2}{\phi(v_*)c\tau}, \frac{-bcd_2 + 2\sqrt{d_1 d_2 c(1-bc)}}{\phi(v_*)c}\}$, then (u_*, v_*) is locally asymptotically stable.

(ii) If $\chi < \frac{-bcd_2 - 2\sqrt{d_1 d_2 c(1-bc)}}{\phi(v_*)c}$ or $\frac{-bcd_2 + 2\sqrt{d_1 d_2 c(1-bc)}}{\phi(v_*)c} < \chi < \frac{d_1 + d_2}{\phi(v_*)c\tau}$, then there is Turing instability with the critical wave number $k^2 = k_c^2 = \sqrt{\frac{c(1-bc)}{d_1 d_2}}$.

Remark 2. To ensure the existence of the Turing instability, it is necessary to guarantee $T_k(\tau, \chi) < 0$ and $D_k(\tau, \chi) < 0$ for some $k \in \mathbb{N}_0/\{0\}$. However, $D_k(\tau, \chi) > 0$ always holds for all $k \in \mathbb{N}_0/\{0\}$ and $\chi > 0$. This means that the Turing instability exists only for $\chi < 0$.

B. Numerical simulation

Note that $\phi(v)$ is the density function of the species v, and we will choose different types of $\phi(v)$ to carry out the numerical simulations.

1. $\phi(v)$ takes the linear form

If one takes $\phi(v) = v$, then $\phi(v_*) = 1 - bc > 0$. In the sequel, choosing $b = 1$, $c = 0.7$, $d_1 = 0.95$, and $d_2 = 1.5$, then one has $0 < \tau < 3.3333$, $\frac{d_1 + d_2}{\phi(v_*)c\tau} = 7.7778$, $\frac{-bcd_2 - 2\sqrt{d_1 d_2 c(1-bc)}}{\phi(v_*)c} = -10.2099$,

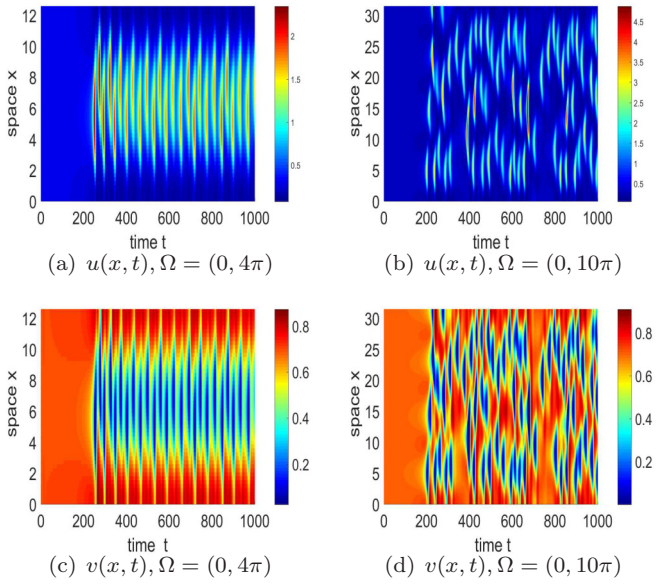

(a) $u(x,t), \Omega = (0, 4\pi)$ (b) $u(x,t), \Omega = (0, 10\pi)$

(c) $v(x,t), \Omega = (0, 4\pi)$ (d) $v(x,t), \Omega = (0, 10\pi)$

FIG. 1. Irregular stripe patterns emerging in the model (14) with linear form density function $\phi(v) = v$ and different spatial lengths. Parameters are $b = 1$, $c = 0.7$, $d_1 = 0.95$, $d_2 = 1.5$, $\tau = 1.5$, and $\chi = -12$.

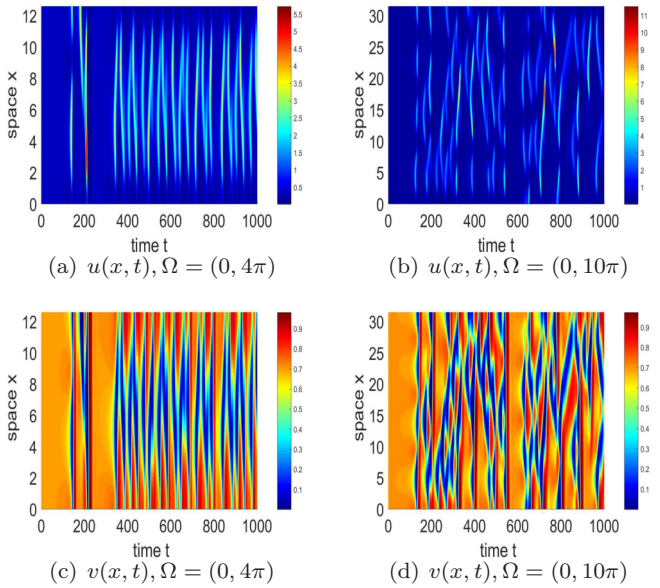

(a) $u(x,t), \Omega = (0, 4\pi)$ (b) $u(x,t), \Omega = (0, 10\pi)$

(c) $v(x,t), \Omega = (0, 4\pi)$ (d) $v(x,t), \Omega = (0, 10\pi)$

FIG. 2. Irregular stripe patterns emerging in the model (14) with linear form density function $\phi(v) = v$ and different spatial lengths. Parameters are $b = 1$, $c = 0.7$, $d_1 = 0.75$, $d_2 = 1.35$, $\tau = 1.5$, and $\chi = -14$.

and $\frac{-bcd_2+2\sqrt{d_1d_2c(1-bc)}}{\phi(v_*)c} = 0.2099$. To display the pattern formation due to the Turing instability, we choose $1.5 = \tau \in (0, 3.3333)$, $-12 = \chi < -10.2099$. Our numerical results show that there are spatial patterns; see Fig. 1. To be precise, in Figs. 1(a) and 1(b) we take the bounded domain $\Omega = (0, 4\pi)$. We then find that there are regular stripe patterns emerging in the bounded region. In fact, there are periodic oscillation patterns. However, with the increase of the spatial lengths, namely keeping $\Omega = (0, 10\pi)$, these regular periodic oscillation patterns will be broken and the irregular spatiotemporal oscillation patterns will occupy the whole bounded domains; see (c) and (d) in Fig. 1. This means that the spatial length will affect the pattern formation of the model. Then, (ii) in Theorem 2 is valid.

In what follows, let us continuously check the validity of Theorem 2 with different parameters. To this end, let us fix $b = 1$, $c = 0.7$, $d_1 = 0.75$, and $d_2 = 1.35$. Then one has $0 < \tau < 3.3333$, $\frac{d_1+d_2}{\phi(v_*)c\tau} = 6.6667$, $\frac{-bcd_2-2\sqrt{d_1d_2c(1-bc)}}{\phi(v_*)c} = -8.8916$, and $\frac{-bcd_2+2\sqrt{d_1d_2c(1-bc)}}{\phi(v_*)c} = -0.1084$. To display the Turing pattern, we still choose the time delay parameter $1.5 = \tau \in (0, 3.3333)$ and take $-14 = \chi < -8.8916$. Our numerical experiments show that there are regular periodic oscillation patterns in pictures (a) and (b) for $\Omega = (0, 4\pi)$, while pictures (c) and (d) display the irregular spatiotemporal oscillation patterns in the domain $\Omega = (0, 10\pi)$ of the model; see Fig. 2. Clearly, we have found the Turing patterns of the reaction-diffusion-chemotaxis model (14), so Theorem 2 is also valid under these parameter values.

2. $\phi(v)$ takes the saturated form

The saturated form $\phi(v)$ takes the form $\phi(v) = \frac{v}{1+\epsilon v^m}$ with $\epsilon > 0$ and $m \geqslant 1$. For simplicity, in this subsection we set $\epsilon = 1$ and $m = 1$. Equation (14) then becomes

$$\begin{aligned} \frac{\partial u}{\partial t} &= d_1 \Delta u + u(1 - bu - v_\tau), \\ \frac{\partial v}{\partial t} &= d_2 \Delta v - \chi \nabla \cdot \left(\frac{v}{1+v} \nabla u \right) + v(u - c). \end{aligned} \tag{15}$$

To carry out the numerical simulations, we choose $b = 1$, $c = 0.7$, $d_1 = 0.85$, and $d_2 = 1.5$. Then one has $0 < \tau < 3.3333$, $b^2cd_2 - 4d_1(1 - bc) = 0.03 > 0$, $\frac{d_1+d_2}{\phi(v_*)c\tau} = 7.4603$, $\frac{-bcd_2-2\sqrt{d_1d_2c(1-bc)}}{\phi(v_*)c} = -12.9065$, and $\frac{-bcd_2+2\sqrt{d_1d_2c(1-bc)}}{\phi(v_*)c} = -0.0935$. To find the Turing patterns of the model (15), one takes $1.6 = \tau \in (0, 3.3333)$, $-16 = \chi < \chi_5$. Numerical results show that the model (15) enjoys regular stripe patterns in the bounded domain $\Omega = (0, 18\pi)$; see Fig. 3. Clearly, they are spatial patterns induced by the Turing instability.

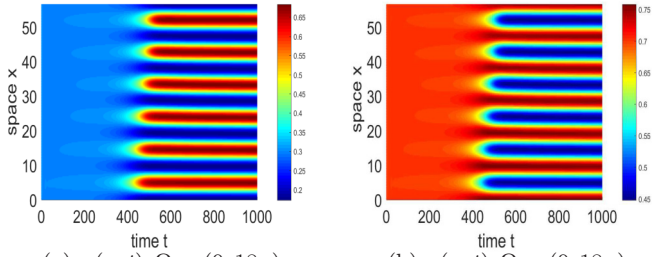

(a) $u(x,t), \Omega = (0, 18\pi)$ (b) $v(x,t), \Omega = (0, 18\pi)$

FIG. 3. Regular stripe patterns emerging in the model (15) with saturated form density function $\phi(v) = \frac{v}{1+v}$ and spatial domain $\Omega = (0, 18\pi)$. Parameters are $b = 1$, $c = 0.7$, $d_1 = 0.85$, $d_2 = 1.5$, $\tau = 1.6$, and $\chi = -16$.

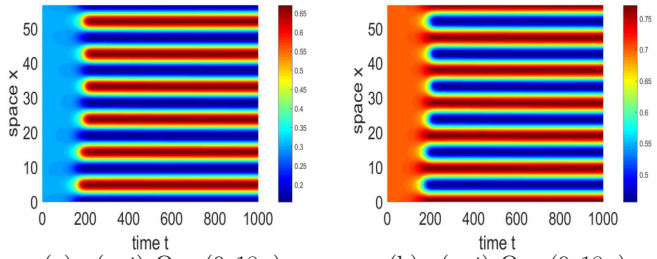

(a) $u(x,t), \Omega = (0, 18\pi)$ (b) $v(x,t), \Omega = (0, 18\pi)$

FIG. 4. Regular stripe patterns emerging in the model (16) with Ricker form density function $\phi(v) = ve^{-v}$ and spatial domain $\Omega = (0, 18\pi)$. Parameters are $b = 1$, $c = 0.7$, $d_1 = 0.85$, $d_2 = 1.45$, $\tau = 1.5$, and $\chi = -17.5$.

3. $\phi(v)$ takes the Ricker form

If the density function $\phi(v)$ is in the Ricker form, then $\phi(v) = ve^{-\epsilon v}$ with $\epsilon > 0$. If $\epsilon = 1$, then $\phi(v) = ve^{-v}$. In this fashion, the delayed reaction-diffusion-chemotaxis model (14) takes the form

$$\begin{aligned}\frac{\partial u}{\partial t} &= d_1\Delta u + u(1 - bu - v_\tau),\\ \frac{\partial v}{\partial t} &= d_2\Delta v - \chi\nabla\cdot(ve^{-v}\nabla u) + v(u - c).\end{aligned} \tag{16}$$

Taking the parameters $b = 1$, $c = 0.7$, $d_1 = 0.85$, $d_2 = 1.45$, and $\Omega = (0, 18\pi)$, we get $0 < \tau < 3.3333$, $\frac{d_1+d_2}{\phi(v_*)c\tau} = 7.316$, $\frac{-bcd_2-2\sqrt{d_1d_2c(1-bc)}}{\phi(v_*)c} = -13.0647$, and $\frac{-bcd_2+2\sqrt{d_1d_2c(1-bc)}}{\phi(v_*)c} = 0.0161$. To observe the Turing patterns of the model (16), one chooses $1.5 = \tau \in (0, 3.3333)$, $-17.5 = \chi < -13.0647$. As a result, numerical results illustrate that model (16) admits the Turing pattern with regular stripe patterns; see Fig. 4. Consequently, the theoretical prediction is valid. Unlike Fig. 3, we find that the growth rate of the stripe patterns in Fig. 4 is faster than Fig. 3 in the same bounded domain Ω.

In short, numerical results confirm the theoretical analysis, and the Turing patterns appear in the delayed reaction-diffusion-chemotaxis predator-prey model with different density functions of $\phi(v)$.

C. Delayed phytoplankton-zooplankton model with chemotaxis

In this subsection, we focus on the following toxin-producing phytoplankton-zooplankton model with time delay and chemotaxis:

$$\begin{aligned}\frac{\partial u}{\partial t} &= d_1\Delta u + ru\Big(1 - \frac{u}{K}\Big) - \alpha uv,\\ \frac{\partial v}{\partial t} &= d_2\Delta v - \chi\nabla\cdot[\phi(v)\nabla u] + (\beta - \theta)uv - dv_\tau,\\ \frac{\partial u}{\partial v} &= \frac{\partial v}{\partial v} = 0,\\ u(x,t) &= u_0(x,t) \geqslant 0,\\ v(x,t) &= v_0(x,t) \geqslant 0,\end{aligned} \tag{17}$$

where u and v describe the densities of the phytoplankton and zooplankton, respectively; parameters r is the intrinsic growth rate of the phytoplankton u; K presents the environmental carrying capacity of u; α is the maximum consumption rate for zooplankton v; β means the ratio of biomass conversion; d is the natural death rate of the zooplankton v; and θ describes the rate of toxic substances produced per unit biomass of phytoplankton. Note that the natural death of the zooplankton species in the real environment needs some time; we employ the term $-dv_\tau$ to describe this aspect. Moreover, the term $-\chi\nabla\cdot[\phi(v)\nabla u]$ is the chemotaxis term with $\chi > 0$ or $\chi < 0$.

Now direct computation shows that the model (17) has a unique positive equilibrium $(u_*, v_*) = (\frac{d}{\beta-\theta}, \frac{r[K(\beta-\theta)-d]}{\alpha(\beta-\theta)K})$ with $0 < \theta < \beta$ and $0 < d < (\beta - \theta)K$. Denoting $f(u, v) = ru(1 - \frac{u}{K}) - \alpha uv$ and $g(u, v) = \beta uv - dv - \theta uv$, then at the positive equilibrium (u_*, v_*) one obtains $f_u = -\frac{r}{K}u_*$, $f_v = -\alpha u_*$, $g_u = (\beta - \theta)v_*$, and $g_v = 0$. Take the transformation $v(x, t - \tau) = v(x, t) - \tau\frac{\partial v(x,t)}{\partial t}$. Then, putting it into model (17), we get the linearized form of model (17) as follows:

$$\begin{aligned}\frac{\partial u}{\partial t} &= d_1\Delta u - \frac{ru_*}{K}u - \alpha u_*v,\\ (1 - d\tau)\frac{\partial v}{\partial t} &= d_2\Delta v - \chi\phi(v_*)\Delta u + (\beta - \theta)v_*u.\end{aligned}$$

Consequently, we have $A_\tau = \left(\begin{smallmatrix}1 & 0\\ 0 & 1-d\tau\end{smallmatrix}\right)$, and

$$D = \begin{pmatrix} d_1\Delta & 0\\ -\chi\phi(v_*)\Delta & d_2\Delta\end{pmatrix},\ J_0 = \begin{pmatrix} -\frac{r}{K}u_* & -\alpha u_*\\ (\beta - \theta)v_* & 0\end{pmatrix}.$$

Using a similar technique, one obtains the characteristic equation

$$\lambda_k^2 - T_k(\tau, \chi)\lambda_k + D_k(\tau, \chi) = 0,\ k \in \mathbb{N}_0,$$

where

$$\begin{aligned}T_k(\tau, \chi) &= -\frac{[(1 - d\tau)d_1 + d_2]k^2 + \frac{r}{K}u_*(1 - d\tau)}{1 - d\tau},\\ D_k(\tau, \chi) &= \frac{d_1d_2k^4 + \big[\frac{r}{K}u_*d_2 + \alpha\chi\phi(v_*)u_*\big]k^2 + \alpha u_*v_*(\beta - \theta)}{1 - d\tau}.\end{aligned}$$

If $k = 0$, one has

$$\lambda_0^2 - T_0(\tau, \chi)\lambda_0 + D_0(\tau, \chi) = 0,$$

where

$$T_0(\tau, \chi) = -\frac{r}{K}u_* < 0,\ D_0(\tau, \chi) = \frac{\alpha u_*v_*(\beta - \theta)}{1 - d\tau}.$$

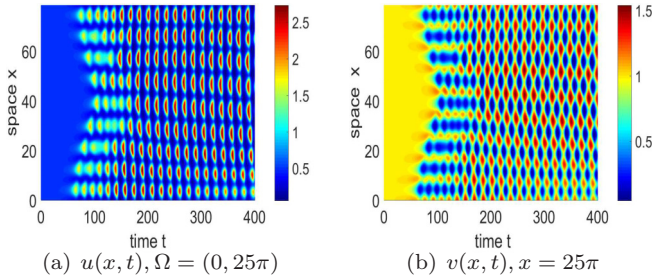

(a) $u(x,t), \Omega = (0, 25\pi)$ (b) $v(x,t), x = 25\pi$

FIG. 5. Reaction-diffusion-chemotaxis model (18) admits the spot patterns in the domain $\Omega = (0, 25\pi)$. Parameters are $\theta = 0.5$, $\beta = 1$, $\alpha = 0.5$, $K = 2$, $r = 0.5$, $d = 0.5$, $d_1 = 0.35$, $d_2 = 1.5$, $\tau = 0.85$, and $\chi = -13$.

Therefore, the unique positive equilibrium $(u_*, v_*) = (\frac{d}{\beta-\theta}, \frac{r[K(\beta-\theta)-d]}{\alpha(\beta-\theta)K})$ for the nondiffusive model of (17) is locally asymptotically stable if we restrict $0 < \tau < \frac{1}{d}$. In this fashion, it is true that $T_k < 0$ for all $k \in \mathbb{N}_0/\{0\}$. On the other hand, by direct calculation, we get $f_v(d_1 g_v + d_2 f_u) = \frac{\alpha r u_*^2 d_2}{K} > 0$ and $f_v = -\alpha u_* < 0$.

Similarly, based on Theorem 1, we have the following.

Theorem 3. For the reaction-diffusion-chemotaxis model (17), let $0 < \theta < \beta$, $0 < d < (\beta - \theta)K$, and

$$0 < \tau < \frac{1}{d}.$$

We have the following:

(i) If $\frac{-ru_*d_2 - 2K\sqrt{d_1 d_2 \alpha u_* v_*(\beta-\theta)}}{\alpha u_* \phi(v_*) K} < \chi < \frac{-ru_*d_2 + 2K\sqrt{d_1 d_2 \alpha u_* v_*(\beta-\theta)}}{\alpha u_* \phi(v_*) K}$, then (u_*, v_*) is locally asymptotically stable.

(ii) If $\chi < \frac{-ru_*d_2 - 2K\sqrt{d_1 d_2 \alpha u_* v_*(\beta-\theta)}}{\alpha u_* \phi(v_*) K}$ or $\chi > \frac{-ru_*d_2 + 2K\sqrt{d_1 d_2 \alpha u_* v_*(\beta-\theta)}}{\alpha u_* \phi(v_*) K}$, then there is Turing instability with the critical wave number $k^2 = k_c^2 = \sqrt{\frac{\alpha u_* v_* (\beta-\theta)}{d_1 d_2}}$.

D. Numerical simulation

In this subsection, we shall check the validity of Theorem 3. We only give the numerical results for the case of $\phi(v) = v$ since similar Turing patterns can be observed by choosing different $\phi(v)$. Accordingly, we get the following model:

$$\begin{aligned} \frac{\partial u}{\partial t} &= d_1 \Delta u + ru\left(1 - \frac{u}{K}\right) - \alpha u v, \\ \frac{\partial v}{\partial t} &= d_2 \Delta v - \chi \nabla \cdot (v \nabla u) + (\beta - \theta) u v - d v_\tau. \end{aligned} \tag{18}$$

Taking the parameters $\theta = 0.5$, $\beta = 1$, $\alpha = 0.5$, $K = 2$, $r = 0.5$, $d = 0.5$, $d_1 = 0.35$, and $d_2 = 1.5$, one obtains the unique positive equilibrium $(u_*, v_*) = (1, 0.5)$ and $\frac{1}{d} = 2$, $\frac{-ru_*d_2 - 2K\sqrt{d_1 d_2 \alpha u_* v_*(\beta-\theta)}}{\alpha u_* \phi(v_*) K} = -3.5494 < 0$, and $\frac{-ru_*d_2 + 2K\sqrt{d_1 d_2 \alpha u_* v_*(\beta-\theta)}}{\alpha u_* \phi(v_*) K} = 0.5494 > 0$. By using (ii) in Theorem 3, we take the chemotaxis coefficient $-13 = \chi < -3.5494$ and time delay control parameter $0.85 = \tau \in (0, 2)$. Our numerical simulation result shows that there is a spot pattern emerging in the delayed reaction-diffusion-chemotaxis model (18); see Fig. 5. The spot shape implies that the pattern is temporally and spatially periodically oscillating. This is different from the pattern formation in Figs. 1–4. Figure 6 illustrates the space oscillation diagrams of the solution (u, v) with different spatial lengths. Overall, conclusion (ii) is true in Theorem 3.

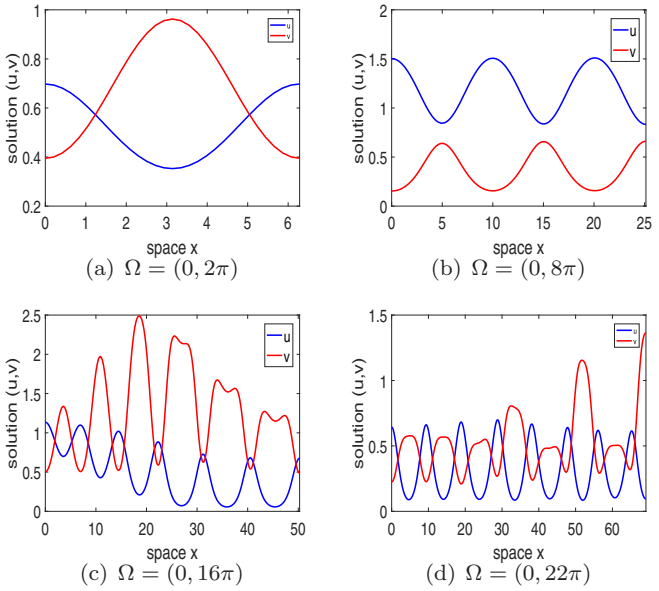

(a) $\Omega = (0, 2\pi)$ (b) $\Omega = (0, 8\pi)$

(c) $\Omega = (0, 16\pi)$ (d) $\Omega = (0, 22\pi)$

FIG. 6. Space oscillation diagrams of the solution (u, v) with different spatial lengths at $t = 400$. Parameters are $\theta = 0.5$, $\beta = 1$, $\alpha = 0.5$, $K = 2$, $r = 0.5$, $d = 0.5$, $d_1 = 0.35$, $d_2 = 1.5$, $\tau = 0.85$, and $\chi = -13$.

In the sequel, we take the parameters $\theta = 0.5$, $\beta = 1$, $\alpha = 0.5$, $K = 2$, $r = 1.25$, $d = 0.5$, $d_1 = 0.35$, and $d_2 = 1.5$. One then obtains the unique positive equilibrium $(u_*, v_*) = (1, 1.25)$ and $\frac{1}{d} = 2$, $\frac{-ru_*d_2 - 2K\sqrt{d_1 d_2 \alpha u_* v_*(\beta-\theta)}}{\alpha u_* \phi(v_*) K} = -2.7961 < 0$, and $\frac{-ru_*d_2 + 2K\sqrt{d_1 d_2 \alpha u_* v_*(\beta-\theta)}}{\alpha u_* \phi(v_*) K} = -0.2039 < 0$. To confirm the validity of (ii) in Theorem 3, we take the chemotaxis coefficient $-8.5 = \chi < -2.7961$ and time delay control parameter $0.5 = \tau \in (0, 2)$. Our simulation result shows that there is a regular stripe pattern in the domain $\Omega = (0, 10\pi)$ of the delayed reaction-diffusion-chemotaxis model (18); see Fig. 7 for details. Similarly, Fig. 8 demonstrates the space oscillation diagrams of the solution (u, v) with different

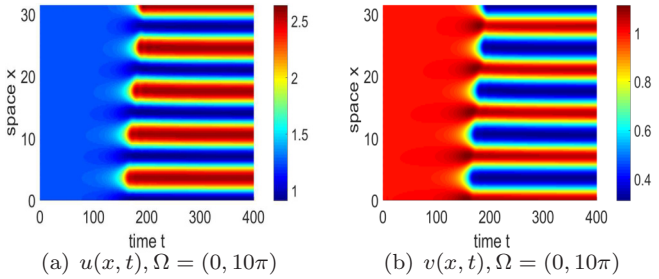

(a) $u(x,t), \Omega = (0, 10\pi)$ (b) $v(x,t), \Omega = (0, 10\pi)$

FIG. 7. Reaction-diffusion-chemotaxis model (18) enjoys the regular stripe patterns in the domain $\Omega = (0, 10\pi)$. Parameters are $\theta = 0.5$, $\beta = 1$, $\alpha = 0.5$, $K = 2$, $r = 1.25$, $d = 0.5$, $d_1 = 0.35$, $d_2 = 1.5$, $\tau = 0.5$, and $\chi = -8.5$.

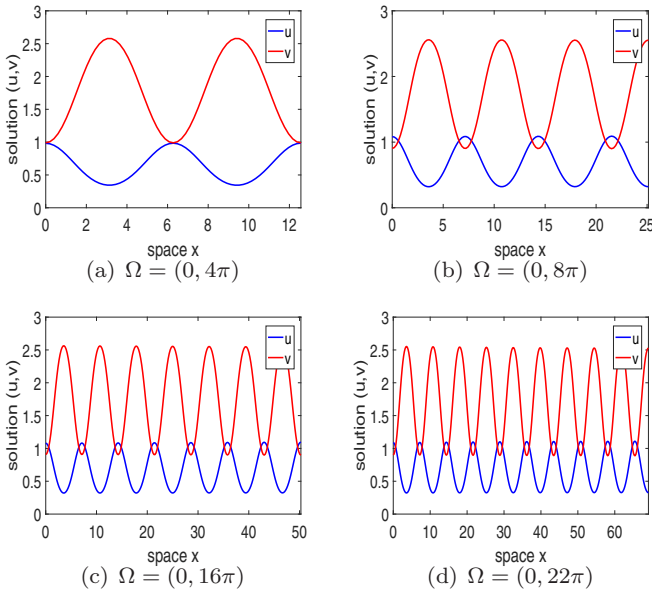

(a) $\Omega = (0, 4\pi)$ (b) $\Omega = (0, 8\pi)$

(c) $\Omega = (0, 16\pi)$ (d) $\Omega = (0, 22\pi)$

FIG. 8. Space oscillation diagrams of the solution (u, v) with different spatial lengths at $t = 400$. Parameters are $\theta = 0.5$, $\beta = 1$, $\alpha = 0.5$, $K = 2$, $r = 0.5$, $d = 0.5$, $d_1 = 0.35$, $d_2 = 1.5$, $\tau = 0.5$, and $\chi = -8.5$.

spatial lengths. Hence, conclusion (ii) is also valid in Theorem 3.

Up to now, we have confirmed that our theoretical results are valid by employing the delayed-chemotaxis-type predator-prey and phytoplankton-zooplankton models as two examples. The numerical results are found to be in good agreement with the theoretical analysis. The Turing instability could emerge in the delayed chemotaxis models when we control the ranges of the parameters τ and χ. Importantly, we can explain that there is no pattern formation in these two systems when time delay and chemotaxis are absent. This implies that delay and chemotaxis effects play a crucial role in inducing the pattern dynamics of reaction-diffusion systems.

IV. CONCLUSIONS

This paper focuses on Turing instability for general delayed reaction-diffusion-chemotaxis models with no-flux boundary conditions. The models admit the term $-\nabla \cdot [\chi\phi(v)\nabla u]$ with the chemotaxis coefficient χ and the delay term $f(u(x, t-\tau), v(x, t-\tau))$ and $g(u(x, t-\tau), v(x, t-\tau))$ with time delay control parameter τ, where $\phi(v)$ is the general density or concentration function. By classifying the parameter range of the chemotaxis coefficient χ and time delay τ, we yield sufficient conditions of the Turing instability of the general delayed reaction-diffusion-chemotaxis models; see Theorem 1. In particular, we can show that time delay parameter τ and chemotaxis parameter χ, respectively, govern the stability of the positive equilibrium for ODEs and PDEs. In what follows, we give two examples to check the validity of the theoretical analysis by employing the predator-prey model and the phytoplankton-zooplankton model with time delay and chemotaxis, respectively. It is found that these two models enjoy Turing instability, and spatial patterns are also illustrated in the numerical simulations; see Figs. 1–8. Consequently, theoretical results are valid and useful for investigating the Turing instability of the delayed reaction-diffusion-chemotaxis models.

ACKNOWLEDGMENTS

The authors are very grateful to the referees for their detailed comments and valuable suggestions, which greatly improved the present manuscript. This work was supported by the National Natural Science Foundation of China (No. 11971032) and funded by China Postdoctoral Science Foundation (No. 2021M701118).

[1] A. M. Turing, The chemical basis of morphogenesis, Philos. Trans. R. Soc. London **237**, 37 (1952).
[2] M. X. Chen, R. C. Wu, and L. P. Chen, Pattern dynamics in a diffusive Gierer-Meinhardt model, Int. J. Bifurcation Chaos **30**, 2030035 (2020).
[3] R. A. Van Gorder, V. Klika, and A. L. Krause, Turing conditions for pattern forming systems on evolving manifolds, J. Math. Biol. **82**, 4 (2021).
[4] T. Butler and N. Goldenfeld, Fluctuation-driven Turing patterns, Phys. Rev. E **84**, 011112 (2011).
[5] Z. Z. Xiang, J. Li, P. You *et al.*, Turing patterns with high-resolution formed without chemical reaction in thin-film solution of organic semiconductors, Nat. Commun. **13**, 7422 (2022).
[6] D. Hernandez-Aristizabal, D. A. G. Alvarado, and A. Madzvamuse, Turing pattern formation under heterogeneous distributions of parameters for an activator-depleted reaction model, J. Nonlin. Sci. **31**, 34 (2021).
[7] A. Marciniak-Czochra, G. Karch, and K. Suzuki, Instability of turing patterns in reaction-diffusion-ODE systems, J. Math. Biol. **74**, 583 (2017).
[8] O. P. Yadav and R. Jiwari, A finite element approach to capture Turing patterns of autocatalytic Brusselator model, J. Math. Chem. **57**, 769 (2019).
[9] S. Subramanian and S. M. Murray, Pattern selection in reaction diffusion systems, Phys. Rev. E **103**, 012215 (2021).
[10] M. X. Chen, R. C. Wu, and X. H. Wang, Non-constant steady states and Hopf bifurcation of a species interaction model, Commun. Nonlin. Sci. Numer. Simul. **116**, 106846 (2023).
[11] M. Asllani, J. D. Challenger, and F. S. Pavone, The theory of pattern formation on directed networks, Nat. Commun. **5**, 4517 (2014).
[12] Q. An and W. H. Jiang, Bifurcations and spatiotemporal patterns in a ratio-dependent diffusive Holling-Tanner system with time delay, Math. Meth. Appl. Sci. **42**, 440 (2019).
[13] Q. Hu and J. W. Shen, Delay-induced self-organization dynamics in a prey-predator network with diffusion, Nonlin. Dyn. **108**, 4499 (2022).
[14] J. T. Zhao and J. J. Wei, Persistence, Turing instability and Hopf bifurcation in a diffusive plankton system with delay and quadratic closure, Int. J. Bifurcation Chaos **26**, 1650047 (2016).

[15] F. Q. Yi, E. A. Gaffney, and S. Seirin-Lee, The bifurcation analysis of turing pattern formation induced by delay and diffusion in the Schnakenberg system, Discret. Contin. Dyn. Syst. B **22**, 647 (2017).

[16] S. Mishra and R. K. Upadhyay, Spatial pattern formation and delay induced destabilization in predator-prey model with fear effect, Math. Meth. Appl. Sci. **45**, 6801 (2022).

[17] E. F. Keller and L. A. Segel, Initiation of slime mold aggregation viewed as an instability, J. Theor. Biol. **26**, 399 (1970).

[18] M. X. Chen and R. C. Wu, Dynamics of a harvested predator-prey model with predator-taxis, Bull. Malays. Math. Sci. Soc. **46**, 76 (2023).

[19] M. Winkler, Finite-time blow-up in low-dimensional Keller-Segel systems with logistic-type superlinear degradation, Z. Angew. Math. Phys. **69**, 40 (2018).

[20] Y. Z. Han, Z. F. Li, J. C. Tao *et al.*, Pattern formation for a volume-filling chemotaxis model with logistic growth, J. Math. Anal. Appl. **448**, 885 (2017).

[21] Z. A. Wang and T. Hillen, Classical solutions and pattern formation for a volume filling chemotaxis model, Chaos **17**, 037108 (2007).

[22] M. X. Chen and H. M. Srivastava, Stability of bifurcating solution of a predator-prey model, Chaos Solitons Fractals **168**, 113153 (2023).

[23] M. C. Köhnke, I. Siekmann, and H. Malchow, Taxis-driven pattern formation in a predator-prey model with group defense, Ecol. Complex. **43**, 100848 (2020).

[24] J. P. Gao, S. J. Guo, and L. Ma, Global existence and spatiotemporal pattern formation of a nutrient-microorganism model with nutrient-taxis in the sediment, Nonlin. Dyn. **108**, 4207 (2022).

[25] S. Sen, P. Ghosh, S. S. Riaz, and D. S. Ray, Time-delay-induced instabilities in reaction-diffusion systems, Phys. Rev. E **80**, 046212 (2009).

[26] M. Chen and H. M. Srivastava, Existence and stability of bifurcating solution of a chemotaxis model, Proc. Am. Math. Soc. **151**, 4735 (2023).

[27] S. N. Wu, J. P. Shi, and B. Y. Wu, Global existence of solutions and uniform persistence of a diffusive predator-prey model with prey-taxis, J. Diff. Eq. **260**, 5847 (2016).

[28] R. Tyson, S. R. Lubkin, and J. D. Murray, Model and analysis of chemotactic bacterial patterns in a liquid medium, J. Math. Biol. **38**, 359 (1999).

[29] J. M. Lee, T. Hillena, and M. A. Lewis, Continuous traveling waves for prey-taxis, Bull. Math. Biol. **70**, 654 (2008).

[30] J. P. Previte and K. A. Hoffman, Period doubling cascades in a predator-prey model with a scavenger, SIAM Rev. **55**, 523 (2013).